The 1st Joint International Conference on Multibody System Dynamics
May 25–27, 2010, Lappeenranta, Finland

A Non-Incremental Finite Element Formulation Of Large Deformation Piezoceramic-Laminated-Plates

Ahmed M. El-Assal[*], **Ayman A. Nada**[#]

[*] Benha Institute of Technology
Benha University
Benha,13512 , Egypt
e-mail: amelassal@yahoo.com

[#] College of Engineering
Jazan University
Jazan, 21981, KSA
e-mail: arobust@tedata.net.eg

ABSTRACT

This investigation presents an electromechanically coupled non-incremental finite element formulation of large deformation piezo-laminated structures. It concerns a way to generate new finite element in the Absolute Nodal Coordinate Formulation (ANCF) for laminated composite rectangular plates. This formulation utilizes the assumption that the bonds between the laminae are infinitesimally thin and shear nondeformable. Using the expressions for the kinetic and strain energies, the mass matrix and the elastic forces are identified. In the ANCF, the nodal coordinates consist of absolute position coordinates and gradients that can be used to define a unique rotation and deformation fields within the element. As a result, the cross section is allowed to deform and it is no longer treated as a rigid surface and therefore, leads to a new set of modes referred as the ANCF-coupled deformation modes. In this paper, the ANCF-coupled deformation modes are identified and eliminated in such a way to achieve the continuity of the remaining gradients at the nodal points, and obtain a formulation that automatically satisfies the principle of work and energy. Convergence and accuracy of the finite element ANCF-Piezo-Laminated-Plate is demonstrated in geometrically nonlinear static and dynamic test problems, as well as in linear analysis of natural frequencies. The computer implementation and several numerical examples are presented in order to demonstrate the use of the formulation developed in this paper. A comparison with the commercial finite element package COMSOL MULTIPHYSICS [5] is carried out with a good agreement.

Keywords: Smart structure, Absolute nodal coordinate formulation, Plate element, Large deformation.

1 INTRODUCTION

With the increasing use of piezoelectric materials as actuators or sensors in smart structures and other applications, there is a growing need for accurate models that give reliable results for laminated composite plate structures. A wide variety of different approaches for the finite element modeling of piezoelectric beam, plate and shell structures can be found in the literature. A survey of the finite element modeling of piezoelectric actuators and sensors for smart structures has been given by [2], in which attention is given to the finite element formulations that have been developed for solids, shells, plates and beams. Descriptions of the elements' characteristics, geometry, independent variables, interpolation functions and degrees of freedom are given. The review article [15] makes a classification of the proposed theories for the analysis of piezoelectric adaptive laminated structures into the *ESL* model and the *layerwise* model. In the *ESL* models, the laminate is assumed to deform as a single layer, assuming a smooth variation of the displacement field across the thickness. The formulations based on this approach are therefore denoted as equivalent single-layer models (*ESL* models). The kinematics of the elements are commonly based either on the Kirchhoff or the Reissner–Mindlin assumptions, which leads for elastic elements to the classical laminate theory or the first-order shear deformation theory (FSDT). The kinematic degrees of freedom are defined only at the mid-surface of the laminate, not for every layer. In the *layerwise* models, a smooth variation of the kinematic variables is assumed within each layer, but the displacement field across the thickness of the laminate is not smooth at the interfaces of the layers. This leads to the so called layerwise or zig-zag laminate theories, as described in [3, 4]. These theories yield more accurate results especially for thick laminates and are better suited to predict interlaminar effects, but they lead to an increased overall number of degrees of freedom for the finite element model as compared to the equivalent single-layer theories [19]. Large number of recent publications are found in [10, 11, 12, 20].

Most of the existing quadrilateral plate elements for geometrically nonlinear analysis of laminated composite plates are FSDT-based because of its simplicity of formulation and low computational cost of FSDT. FSDT can predict most of the structural behavior adequately together with proper shear correction factors [6]. The authors in [9] employed the classical laminate theory with the induced actuation and variational principles to formulate equations of motion. The plate element without the electro-mechanical coupling was developed. The total charge on the sensor layer was calculated from the direct piezoelectric equation. In order to model structures with complex geometry, isoparametric hexahedron and tetrahedral solid elements were developed for piezoceramic structures [1, 14]. In [8] also presented a finite element formulation with eight-node three dimensional composite brick elements. Large deformation analyses for beam, plate and shell structures with piezoelectric materials have been reported in the literature.

For large flexible space structures such as a solar array, or large space antenna, only the global response, e.g. global deformation, is of interest. The shape and vibration of the structure can be actively compensated and suppressed by the use of bonded/embedded piezoelectric actuators and sensors. However, the *layerwise* models with large computational cost are not convenient for active shape control or active vibration control of large flexible space structures. On the other side, the use of ESL models are derived for a combined isotropic, linearly elastic body and a piezoelectric body undergoing small or large deformations.

The main objective of the present work is to develop an efficient modeling method for laminated composite plates bonded to piezoelectric actuators and sensors, which is suitable for large deformation problems with complex shapes. To this end, the recently developed Absolute Nodal Coordinate Formulation (ANCF) is used [16, 17, 13]. The ANCF is presented for simulation and analysis of the performance of surface-bonded piezoelectric actuators in suppressing non-linear transverse vibrations that are induced by very flexible structures. The elastic deformations experienced are an order of magnitude larger than cases considered to date.

Even with the surface-bonded lead zirconium titanate (PZT) patches, the cross section of the flexible structure is well within the domain of no shearing deformations are considered. The dominant source of non-linearity is a geometric non-linearity due to large curvatures. Therefore, the ANCF of the thin plate element introduced by [7] is implemented with deflections of an order of magnitude larger than those considered in past works.

2 KINEMATICS RELATIONS OF ABSOLUTE NODAL COORDINATE FORMULATION

In the absolute nodal coordinate formulation, the nodal coordinates of the elements are defined in a fixed inertial coordinate system, and consequently no coordinate transformation is required. The element nodal coordinates represent global displacements and slopes, and no infinitesimal or finite rotations are used as nodal coordinates. Furthermore, no assumptions on the magnitude of the element rotations are made. In the absolute nodal coordinate formulation, the global position vector, of an arbitrary point on the plate is defined in terms of the nodal coordinates and the element shape function as:

$$\{r\} = \left\{ \begin{array}{ccc} r_1 & r_2 & r_3 \end{array} \right\}^T = [S]\{e\} \tag{1}$$

where $[S]$ is the element shape function matrix, x, y and z are the local coordinates of the element defined in the element coordinate system and $\{e\}$ is the vector of element nodal coordinates. In equation(1), the plate is described as a continuous volume, making it possible to relax the assumption of rigid cross sections.

For a 4-noded plate element (i, j, m, n), as shown in Figure (1), 12 nodal coordinates can be used for each node. The coordinates of node j, $\{e\}$, can be written as:

$$\{e_j\} = \left\{ \begin{array}{cccc} \{r_j\}^T & \frac{\partial \{r_j\}^T}{\partial x} & \frac{\partial \{r_j\}^T}{\partial y} & \frac{\partial \{r_j\}^T}{\partial z} \end{array} \right\}^T \tag{2}$$

where vector $\{r_j\}$ defines the global position of node j and the three vectors $\partial\{r_j\}/\partial x$, $\partial\{r_j\}/\partial y$, and $\partial\{r_j\}/\partial z$, define the position vector gradients (slopes) at node j . The nodal coordinates of one element can then be given by the vector $\{e_j\}$:

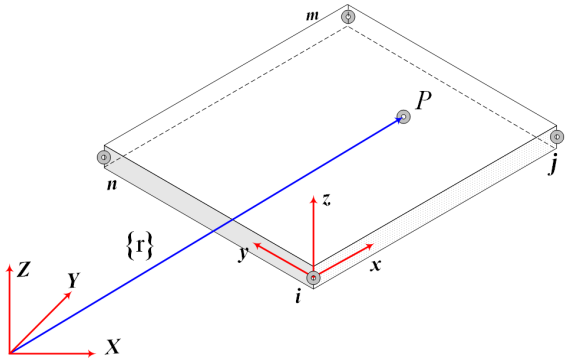

Figure 1. The Four nodes plate element

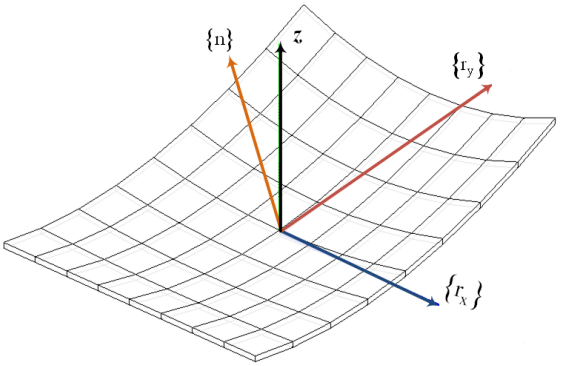

Figure 2. Normal vector

$$\{e\} = \left\{ \{e_i\}^T \quad \{e_j\}^T \quad \{e_m\}^T \quad \{e_n\}^T \right\}^T \tag{3}$$

2.1 Thin Plate Element

For thin plates, the deformation of the element along the thickness direction can be neglected. This leads to reduced set of deformation modes since the displacement field of the element becomes dependent on the spatial coordinates x and y only. In this case, the position vector gradients obtained by differentiation with respect to z are not considered as nodal coordinates, leading to a reduced order element with 36 degrees of freedom. The normal vector $\{n\}$ of the mid surface of the plate can always be defined using cross product of the vectors $\{r_x\}$ and $\{r_y\}$, with subscript x and y refer to partial derivatives with respect to these coordinates, see Figure (2). The Shape functions of the thin plate element can be directly obtained from the shape function matrix of the plate element by omitting the components that depend on the z coordinate [7]. For the reduced order element, the element nodal coordinate vector at node j is defined as follows:

$$\{e_j\} = \left\{ \{r_j\}^T \quad \frac{\partial \{r_j\}^T}{\partial x} \quad \frac{\partial \{r_j\}^T}{\partial y} \right\}^T \tag{4}$$

$$\{r\} = [S(x,y)]\{e\} \tag{5}$$

2.2 Strain Energy

The three-dimensional thin-plate element is based on Kirchhoff's plate theory. Following Kirchhoff theory, the strain energy of a thin plate can be written as the sum of two terms: one term is due to membrane and shear deformations at the plate mid-surface, whereas the other term is due to the plate bending and twist. The strain energy can then be written for a thin plate as follows [7, 17]:

$$\begin{aligned} U_e &= U_e^m + U_e^\kappa \\ &= \frac{1}{2}\int_V \{\varepsilon^m\}^T \left[c^E\right] \{\varepsilon^m\}\, dV + \frac{1}{2}\int_V \{\varepsilon^\kappa\}^T \left[c^E\right] \{\varepsilon^\kappa\}\, dV \end{aligned} \tag{6}$$

Where $\left[c^E\right]$ is the elastic coefficient matrix for homogeneous isotropic material and is defined as:

$$\left[c^E\right] = \frac{E}{1-\nu^2} \begin{bmatrix} 1 & \nu & 0 \\ \nu & 1 & 0 \\ 0 & 0 & (1-\nu)/2 \end{bmatrix} \tag{7}$$

The membrane and shear strain vector $\{\varepsilon^m\}$ is defined as:

$$\{\varepsilon^m\} = \begin{Bmatrix} \varepsilon_{xx} & \varepsilon_{yy} & 2\varepsilon_{xy} \end{Bmatrix}^T \tag{8}$$

where ε_{xx} and ε_{yy} are the normal strain components in x and y direction and ε_{xy} is the shear strain. The curvature strain vector $\{\varepsilon^\kappa\}$ is given by:

$$\{\varepsilon^\kappa\} = z\{\kappa\} \tag{9}$$

The curvature vector $\{\kappa\} = \begin{Bmatrix} \kappa_{xx} & \kappa_{yy} & 2\kappa_{xy} \end{Bmatrix}^T$ can be expressed in terms of the gradient vectors as the following relations [18]:

$$\kappa_{xx} = \frac{\{n\}^T \{r_{xx}\}}{\|\{n\}\|^3},\ \kappa_{yy} = \frac{\{n\}^T \{r_{yy}\}}{\|\{n\}\|^3},\ \ \kappa_{xy} = \frac{\{n\}^T \{r_{xy}\}}{\|\{n\}\|^3} \tag{10}$$

$$\Rightarrow \{\kappa\} = \begin{bmatrix} \frac{\{n\}^T}{\|\{n\}\|^3}[S_{xx}] \\ \frac{\{n\}^T}{\|\{n\}\|^3}[S_{yy}] \\ 2\frac{\{n\}^T}{\|\{n\}\|^3}[S_{xy}] \end{bmatrix} \{e\} = [B(\{e\})]\{e\} \tag{11}$$

The nonlinear matrix $[B(\{e\})]$ can be defined as:

$$[B] = \frac{1}{\|\{n\}\|^3} \begin{bmatrix} \{n\}^T [S_{xx}] \\ \{n\}^T [S_{yy}] \\ 2\{n\}^T [S_{xy}] \end{bmatrix} \tag{12}$$

where $\{n\}$ is the normal to the element mid surface obtained as:$\{n\} = \{r_x\} \times \{r_x\}$, and its norm can be defined as $\|\{n\}\| = \sqrt{\{n\}^T \{n\}}$.

For situations in which the curvature effects dominate the dynamics (low-tension plates) as in the case of piezoelectric laminated plates, one would expect the differences induced by the membrane strain to be quite small and can be neglected. Therefore the coupled deformation modes are eliminated and then the strain energy should take the form of:

$$U_e^\kappa = \frac{1}{2}\int_V \{\varepsilon^\kappa\}^T \left[c^E\right] \{\varepsilon^\kappa\}\, dV = \frac{1}{2}\int_V z^2 \{\kappa\}^T \left[c^E\right] \{\kappa\}\, dV \tag{13}$$

3 PIEZOELECTRIC LAMINATED PLATE

The voltage ϕ_a across the bender element forces the bottom layer to expand, while the upper layer contracts, as depicted in Figure (3). The result of these physical changes is a strong curvature; this implies in a large deflection at the tip when the other end is clamped. The tip deflection may be much larger than the change in length of either ceramic layer. Due to the reciprocity effect, deformation of the sensor will produce a charge across the sensor electrode, which is collected through the sensor surface as an electric voltage ϕ_s.

When only one poling direction is taken into account, the applied or sensed electric potential through the actuator or sensor element is given by the following equation:

$$\{\phi\} = \begin{Bmatrix} \phi_x & \phi_y & \phi_z \end{Bmatrix}^T = \begin{Bmatrix} 0 & 0 & \phi_z \end{Bmatrix}^T = [N_\phi]\ \phi_k \tag{14}$$

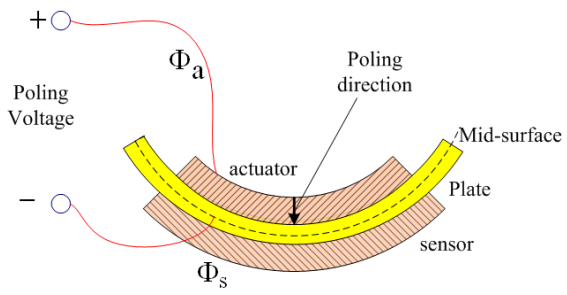

Figure 3. Curvature of a laminated plate

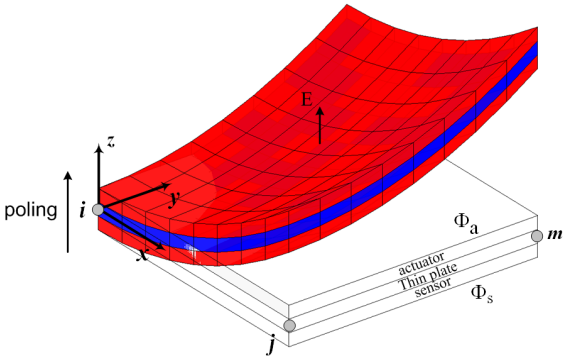

Figure 4. Laminated Piezoelectric ANCF element.

such that:

$$\phi_z = \left(\frac{z - \frac{h_p}{2}}{h_i} \right) \phi_i \tag{15}$$

where h_k and ϕ_k, $(k = a, s)$ are the thickness and the maximum electric potential at the external surface of the corresponding piezoelectric element (actuator and/or sensor), as shown in Figure (4). z (z_a and z_s) is defined over the intervals:

$$\frac{h_p}{2} \leq z_a \leq \frac{h_p}{2} + h_a, \qquad -\frac{h_p}{2} \geq z_s \geq -\frac{h_p}{2} - h_s \tag{16}$$

Assuming that the electric field $\{E\}$ is constant through the actuator and sensor elements thickness; the gradient operators give the electric field of the piezoelectric actuator and sensor layers as:

$$\{E_a\} = -\left[B_{\phi_a}\right] \phi_a, \qquad \{E_s\} = -\left[B_{\phi_s}\right] \phi_s \tag{17}$$

where

$$\left[B_{\phi_a}\right] = \begin{bmatrix} 0 & 0 & \frac{1}{h_a} \end{bmatrix}^T, \qquad \left[B_{\phi_s}\right] = \begin{bmatrix} 0 & 0 & \frac{1}{h_s} \end{bmatrix}^T \tag{18}$$

Constitutive equations: The constitutive relations for piezoelectric materials take the form as:

$$\{\sigma\} = \sum_{k=1}^{3} \left[c_k^E\right] \{\varepsilon_k\} - \sum_{k=1}^{3} [e_k]^T [J] \{E_k\} \tag{19}$$

$$\{D\} = \sum_{k=1}^{3} [e_k] \{\varepsilon_k\} + \sum_{k=1}^{3} [\varsigma_k^\varepsilon] [J] \{E_k\} \tag{20}$$

where $\{\sigma\}$ represents the stress vector, $\{\varepsilon\}$ is the strain vector, $\{E\}$ is the electric field, $\{D\}$ is the electric displacement, $\left[c^E\right]$ is the elastic coefficients at constant $\{E\}$, $[\varsigma^\varepsilon]$ is the dielectric coefficients at constant$\{\varepsilon\}$. $[e]$ is the piezoelectric coupling coefficients. The subscript $k = 1, 2, 3 = a, p, s$ refers to the piezoelectric actuator, plate, and sensor respectively. It should be mentioned here that $[e_p] = \left[\varsigma_p^\varepsilon\right] = [0]$; no electric strength for the plate. The matrix $[J]$ is the transformation matrix due to the large deformation of the element.

3.1 Variational principal

Hamilton's principle is employed here to derive the finite element equations:

$$\int_{t_1}^{t_2} \left[\delta\left(T - U + W_{El}\right) + \delta W_{Ex}\right] dt = 0, \tag{21}$$

where t_1 and t_2 are two arbitrary instants, T is the kinetic energy, U is the potential energy,W_{El} denotes the work done by electrical forces. The total kinetic energy T and the potential energy U of the composite structure are described by the following relations:

$$T = \frac{1}{2}\int_V \rho \left\{\dot{r}\right\}^T \left\{\dot{r}\right\} dV \tag{22}$$

$$U = \frac{1}{2}\int_V \left\{\varepsilon\right\}^T \left\{\sigma\right\} dV \tag{23}$$

where $\{\dot{r}\}$ is the differentiation of $\{r\}$ with respect to the time t ,$\{r\}$ is given by equation (5).The work done by electrical forces is given by Equation (24), where $\{D\}$ is the electric displacement vector, and $\{E\}$ is the electric field.:

$$W_{El} = \frac{1}{2}\int_V \left\{E\right\}^T \left\{D\right\} dV \tag{24}$$

The virtual work of the external forces can be written as:

$$\delta W_{Ex} = \int_V \left\{\delta r\right\}^T \left\{f_b\right\} dV + \int_A \left\{\delta r\right\}^T \left\{f_A\right\} dA - \int_A \left\{\delta\phi\right\}^T \sigma_q dA \tag{25}$$

where f_b is the body force, f_A is the surface force, and σ_q is the surface electrical stress. The element differential volume dV for laminated plate is defined as:

$$dV = \sum_{k=1}^{3} dV_k = dV_a + dV_p + dV_s \tag{26}$$

the subscript p, a and s refer to the plate, actuator and sensor elements, respectively; and defined as follows:

$$dV_a = \int_{(h_p/2)}^{(h_p/2)+h_a} \int_0^b \int_0^a dxdydz, \quad dV_p = \int_{-h_p/2}^{h_p/2} \int_0^b \int_0^a dxdydz, \quad dV_s = \int_{-(h_p/2)-h_s}^{-(h_p/2)} \int_0^b \int_0^a dxdydz \tag{27}$$

Integrating the variational kinetic energy term $\rho\left\{\delta\dot{r}\right\}^T\left\{\dot{r}\right\}$ by parts over the time interval,see Equation (22) one gets:

$$\int_{t_1}^{t_2} \rho\left\{\delta\dot{r}\right\}^T\left\{\dot{r}\right\} dt = \left[\rho\left\{\delta r\right\}^T\left\{\delta\dot{r}\right\}\right]_{t_1}^{t_2} - \int_{t_1}^{t_2} \rho\left\{\delta r\right\}^T\left\{\ddot{r}\right\} dt \tag{28}$$

in which the first term vanishes,$\{\delta r\}$ being equal to zero in $t = t_1$ and $t = t_2$.

By substituting the constitutive equation, Equation (19), into the potential energy term (23), yields:

$$U = \frac{1}{2}\int_{V} \{\varepsilon\}^T \left[c^E\right] \{\varepsilon\}\, dV - \frac{1}{2}\int_{V_a} \{\varepsilon_a\}^T [e_a]^T \{E_a\}\, dV - \frac{1}{2}\int_{V_s} \{\varepsilon_s\}^T [e_s]^T \{E_s\}\, dV \tag{29}$$

and substituting the constitutive equation, Equation (20), in the work done by electrical force, equation (24) yields:

$$\begin{aligned} W_{El} \;=\; & \frac{1}{2}\int_{Va} \{E_a\}^T [e_a] \{\varepsilon\}\, dV_a + \frac{1}{2}\int_{Vs} \{E_s\}^T [e_s] \{\varepsilon\}\, dV_s \\ & + \frac{1}{2}\int_{V_a} \{E_a\}^T [\varsigma_a^{\varepsilon}] \{E_a\}\, dV_a + \frac{1}{2}\int_{V_s} \{E_s\}^T [\varsigma_s^{\varepsilon}] \{E_s\}\, dV_s \end{aligned} \tag{30}$$

therefore, by substituting Equations (28,29,30, 25), into Equation (21) yields:

$$\int_{t_1}^{t_2} \left[\begin{array}{c} -\int_V \rho \{\delta r\}^T \{\ddot{r}\} - \\ \int_V \{\delta\varepsilon\}^T \left[c^E\right] \{\varepsilon\}\, dV + \int_{V_a} \{\delta\varepsilon\}^T [e_a]^T \{E_a\}\, dV_a + \int_{V_s} \{\delta\varepsilon\}^T [e_a]^T \{E_a\}\, dV_s + \\ \int_{V_a} \{E_a\}^T [e_a] \{\varepsilon\}\, dV_a + \int_{V_s} \{E_s\}^T [e_s] \{\varepsilon\}\, dV_s + \\ \int_{V_a} \{E_a\}^T [\varsigma_a^{\varepsilon}] \{E_a\}\, dV_a \int_{V_s} \{E_s\}^T [\varsigma_s^{\varepsilon}] \{E_s\}\, dV_s + \\ \int_A \{\delta r\}^T \{f_A\}\, dA - \int_A \{\delta\phi\}^T \sigma_q dA \end{array} \right] dt = 0 \tag{31}$$

$$\int_{t_1}^{t_2} \left[\begin{array}{l} -\{\delta e\}^T \int_V \rho [S]^T [S]\, dV \{\ddot{e}\} - \{\delta e\}^T \int_V z^2 [B]^T \left[c^E\right] [B]\, dV \{e\} - \\ \{\delta e\}^T \int_{V_a} z [B]^T [e_a]^T \left[B_{\phi_a}\right] dV_a \{\phi_a\} - \{\delta e\}^T \int_{V_s} z [B]^T [e_s]^T \left[B_{\phi_s}\right] dV_s \{\phi_s\} - \\ \{\delta\phi_a\}^T \int_{V_a} z \left[B_{\phi_a}\right]^T [e_a] [B]\, dV_a \{e\} - \{\delta\phi_s\}^T \int_{V_s} z \left[B_{\phi_s}\right]^T [e] [B]\, dV_s \{e\} + \\ \{\delta\phi_a\}^T \int_{V_a} \left[B_{\phi_a}\right]^T [\varsigma_a^{\varepsilon}] \left[B_{\phi_a}\right] dV_a \{\phi_a\} + \{\delta\phi_s\}^T \int_{V_s} \left[B_{\phi_s}\right]^T [\varsigma_s^{\varepsilon}] \left[B_{\phi_s}\right] dV_s \{\phi_s\} + \\ \{\delta e\}^T \int_V [S]^T \{f_b\}\, dV + \{\delta e\}^T \int_A [S]^T \{f_A\}\, dA - \delta \{\phi\}^T \int_A \sigma_q dA \end{array} \right] dt = 0 \tag{32}$$

which must be verified for any arbitrary variation of the displacement $\{\delta e\}$ and electrical potential $\{\delta\phi_i\}$. For an element, equation (32), can be written under the form:

$$\int_{t_1}^{t_2} \left[\begin{array}{l} \{\delta e\}^T \left\{ [M_{ee}] \{\ddot{e}\} + [K_{ee}] \{e\} + \left[K_{e\phi_a}\right] \{\phi_a\} + \left[K_{e\phi_s}\right] \{\phi_s\} - \{F_e\} \right\} + \\ \{\delta\phi_a\}^T \left\{ \left[K_{\phi_a e}\right] \{e\} + \left[K_{\phi_a\phi_a}\right] \{\phi_a\} + \{Q_{ea}\} \right\} + \\ \{\delta\phi_s\}^T \left\{ \left[K_{\phi_s e}\right] \{e\} + \left[K_{\phi_s\phi_s}\right] \{\phi_s\} + \{Q_{es}\} \right\} \end{array} \right] dt = 0, \tag{33}$$

3.2 Element matrices and equations of motion

Allowing arbitrary variations of $\{e\}$ and $\{\phi_k\}$, three equilibrium equations written in absolute coordinates are now obtained for the on the body i,element j,as:

$$\left[M_{ee}^{ij}\right] \left\{\ddot{e}^{ij}\right\} + \left[K_{ee}^{ij}\right] \left\{e^{ij}\right\} + \left[K_{e\phi_a}^{ij}\right] \left\{\phi_a^{ij}\right\} + \left[K_{e\phi_s}^{ij}\right] \left\{\phi_s^{ij}\right\} - \left\{F_e^{ij}\right\} = 0 \tag{34}$$

$$\left[K_{\phi_a e}^{ij}\right]\left\{e^{ij}\right\}+\left[K_{\phi_a \phi_a}^{ij}\right]\left\{\phi_a^{ij}\right\}+\left\{Q_{ea}^{ij}\right\}=0 \tag{35}$$

$$\left[K_{\phi_s e}^{ij}\right]\left\{e^{ij}\right\}+\left[K_{\phi_s \phi_s}^{ij}\right]\left\{\phi_s^{ij}\right\}+\left\{Q_{es}^{ij}\right\}=0 \tag{36}$$

where $\left[M_{ee}^{ij}\right]$ and $\left[K_{ee}^{ij}\right]$ are is the mass and stiffness matrix of the body i, element j, related to the plate absolute nodal coordinates, which can be written as:

$$\left[M_{ee}^{ij}\right]=\int_{V^{ij}} \rho\left[S^{ij}\right]^T\left[S^{ij}\right] dV^{ij} \tag{37}$$

$$\left[K_{ee}^{ij}\right]=\int_{V} z^2\left[B^{ij}\right]^T\left[c^E\right]\left[B^{ij}\right] dV \tag{38}$$

The extended mass matrix of the element i can be written as:

$$\left[M_{ee}^{ij}\right]=\sum_{k=1}^{3}\rho_i\int_{V}\left[S^{ij}\right]^T\left[S^{ij}\right] dV^{ij} \tag{39}$$

where $\rho_1=\rho_a$, $\rho_2=\rho_p$, $\rho_3=\rho_s$.Therefor, the mass matrix of the body i, can be assembled as

$$\left[M_{ee}^{i}\right]=\left[B_2^i\right]^T\sum_{j=1}^{ne}\left[B_1^{ij}\right]^T\left[M_{ee}^{ij}\right]\left[B_1^{ij}\right]\left[B_2^i\right] \tag{40}$$

where ne is the number of elements, $\left[B_1^{ij}\right]$ is the connectivity matrix of element j which is a constant Boolean transformation, $\left[B_2^i\right]$ is boundary conditions linear transformation matrix of the body i. Similarly integrating the nonlinear elastic stiffness matrix $\left[K_{ee}^{ij}\right]$ in the z direction yields:

$$\left[K_{ee}^{ij}\right]=\int_{V} z^2\left[B^{ij}\right]^T\left[c^E\right]\left[B^{ij}\right] dV=\sum_{k=1}^{3}h_k\int_{A}\left[B^{ij}\right]^T\left[c_k^E\right]\left[B^{ij}\right] dA \tag{41}$$

Here, $\left[c_k^E\right]$ is given by $\left[c_a^E\right]$, $\left[c_p^E\right]$ and $\left[c_s^E\right]$, for $(k=1,2,3)$ are calculated by equation (7), for the piezoelectric and plate material properties, respectively. h_k is given by:

$$h_1=h_a\left(\frac{h_p}{2}+\frac{h_a}{2}\right)^2+\frac{h_a^3}{12},\quad h_2=\frac{h_p^3}{12},\quad h_3=h_s\left(\frac{h_p}{2}+\frac{h_s}{2}\right)^2+\frac{h_s^3}{12} \tag{42}$$

The electrical-mechanical coupling nonlinear stiffness matrix $\left[K_{e\phi}^{ij}\right]$ and dielectric stiffness matrix $\left[K_{\phi\phi}^{ij}\right]$ can be written as follows:

$$\left[K_{e\phi_a}^{ij}\right] = -\int_{V_a} z\left[B^{ij}\right]^T\left[e_a\right]^T\left[B_{\phi_a}^{ij}\right] dV_a \tag{43}$$

$$\left[K_{e\phi_s}^{ij}\right] = -\int_{V_s} z\left[B^{ij}\right]^T\left[e_s\right]^T\left[B_{\phi_s}^{ij}\right] dV_s \tag{44}$$

$$\left[K^{ij}_{\phi_a e}\right] = \left[K^{ij}_{e\phi_a}\right]^T, \quad \left[K^{ij}_{\phi_s e}\right] = \left[K^{ij}_{e\phi_s}\right]^T \tag{45}$$

$$\left[K^{ij}_{\phi_a \phi_a}\right] = -\int_{V_a} \left[B^{ij}_{\phi_a}\right]^T [\varsigma^{\varepsilon}_a] \left[B^{ij}_{\phi_a}\right] dV_a \tag{46}$$

$$\left[K^{ij}_{\phi_s \phi_s}\right] = -\int_{V_s} \left[B^{ij}_{\phi_s}\right]^T [\varsigma^{\varepsilon}_s] \left[B^{ij}_{\phi_s}\right] dV_s \tag{47}$$

The electrical-mechanical coupling stiffness matrix $\left[K^{ij}_{e\phi}\right]$ and dielectric stiffness matrix $\left[K^{ij}_{\phi\phi}\right]$ can be assembled as shown in Equation (48,49), where the subscript $(k = 1, 3)$ is for the actuator and sensor respectively.

$$\left[K^{i}_{e\phi_k}\right] = \left[B^{i}_{2}\right]^T \sum_{i=1}^{ne} \left[B^{ij}_{1}\right]^T \left[K^{ij}_{e\phi_k}\right] \left[B^{ij}_{1\phi_k}\right] \left[B^{i}_{2\phi_k}\right] \tag{48}$$

The $\left[B^{ij}_{1\phi_k}\right]$ is the connectivity matrix of piezoelectric elements, $\left[B^{i}_{2\phi_k}\right]$ is electrical boundary conditions that activate the piezoelectric elements.

$$\left[K^{i}_{\phi_k \phi_k}\right] = \left[B^{i}_{2\phi_k}\right]^T \sum_{i=1}^{ne} \left[B^{ij}_{1\phi_k}\right]^T \left[K^{ij}_{\phi_k \phi_k}\right] \left[B^{ij}_{1\phi_k}\right] \left[B^{i}_{2\phi_k}\right] \tag{49}$$

$$\left\{F^{ij}\right\} = \int_V \left[S^{ij}\right]^T \left\{f^{ij}_b\right\} dV + \int_A \left[S^{ij}\right]^T \left\{f^{ij}_A\right\} dA \tag{50}$$

$$\left\{Q^{ij}_e\right\} = \int_A \sigma^{ij}_q dA \tag{51}$$

Solving Equation (35), can be solved for the electrical potential across the piezoelectric actuator and sensor, $\left\{\phi^i_a\right\}$ and $\left\{\phi^i_s\right\}$ as:

$$\left\{\phi^i_a\right\} = -\left[K^{i}_{\phi_a \phi_a}\right]^{-1} \left\{Q^i_{ea}\right\} - \left[K^{i}_{\phi_a \phi_a}\right]^{-1} \left[K^{i}_{\phi_a e}\right] \left\{e^i\right\} \tag{52}$$

Since there is no voltage applied to the piezoelectric sensor, i.e., $\left\{Q^i_{es}\right\} = \{0\}$, so that the electrical potential generated (sensor equation) can be calculated by:

$$\left\{\phi^i_s\right\} = -\left[K^{i}_{\phi_s \phi_s}\right]^{-1} \left[K^{i}_{\phi_s e}\right] \left\{e^i\right\} \tag{53}$$

Substituting the results in the Equation of motions, yields:

$$\begin{aligned} \left[M^i_{ee}\right] \left\{\ddot{e}^i\right\} + \left[K_{el}\right] \left\{e^i\right\} &= \left\{F^i_e\right\} + \left[K^{i}_{e\phi_a}\right] \left[K^{i}_{\phi_a \phi_a}\right]^{-1} \left\{Q^i_{ea}\right\} \\ &= \left\{F^i_e\right\} + \left[K^{i}_{e\phi_a}\right] \left\{\phi^i_a\right\} \end{aligned} \tag{54}$$

Where $[K_{el}]$ is the nonlinear electric stiffness matrix and can be defined as:.

$$\left[K_{el}^{i}\right]=\left[\left[K_{ee}^{i}\right]-\left[K_{e\phi_a}^{i}\right]\left[K_{\phi_a\phi_a}^{i}\right]^{-1}\left[K_{\phi_a e}^{i}\right]-\left[K_{e\phi_s}^{i}\right]\left[K_{\phi_s\phi_s}^{i}\right]^{-1}\left[K_{\phi_s e}^{i}\right]\right] \tag{55}$$

4 NUMERICAL SOLUTION

In order to verify the accuracy of the presented finite element formulation, the numerical results are compared with the software COMSOL MULTIPHYSICS [5]. We use Lagrange shape functions of degree 1 and Hermite shape functions of degree 3, for the finite element discretization of the Kirchhoff-Love mechanical tangential displacements.

4.1 Static Solution

The first validation case is the comparison between the static displacement distribution obtained from the numerical techniques presented. In the upcoming validations a rectangular plate and piezoelectric material with the following characteristics are used, see Table (1):

Properties	Sensor	Actuator	Plate
Material	PZT 5H	PZT 5H	Aluminum
E	107×10^{9}	107×10^{9}	73×10^{9}
ρ	7750	7750	2794
υ	0.33	0.33	0.33
h	2×10^{-3}	2×10^{-3}	2×10^{-3}
$(L_x\times L_y)$	0.1×0.2	0.1×0.2	0.6×0.4

Table 1. Material and geometrical propoerties of plate and piezoelectric

In the case of static solution, the acceleration vector $\left\{\ddot{e}^{i}\right\}$ should be vanished from Equation (54), the equation yields to:

$$\left\{F_{e}^{i}\right\}=\left[K_{el}^{i}\right]\left\{e^{i}\right\}-\left[K_{e\phi_a}^{i}\right]\left\{\phi_{a}^{i}\right\}=\{0\} \tag{56}$$

which can be solved for the nodal coordinates vector $\left\{e^{i}\right\}$ using the Newton-Raphson method that satisfies the equilibrium state.

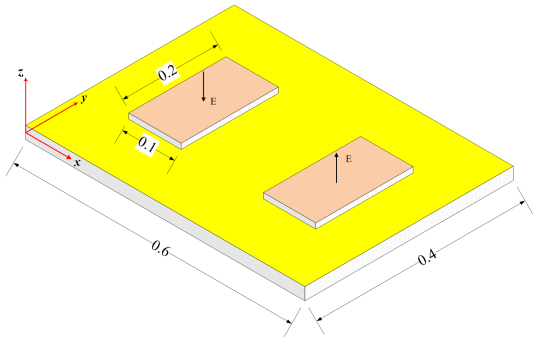

Figure 5. Test configuration

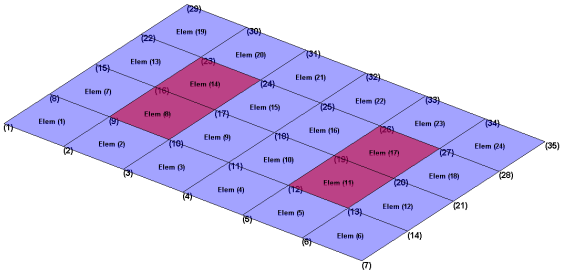

Figure 6. Elements and nodes distribution

The influence of the piezoelectric patches on the static behavior of the structure is investigated. The configuration, illustrated in Figure (5), shows the corresponding layout of the piezoelectric actuators and sensors symmetrically bonded to the plate surfaces. Figure (6) shows the ANCF element distribution and the corresponding nodes, 24 elements are used for this example. Elements numbers 8, 11, 14,17 are laminated piezoelectric plate elements, and piezoelectric properties will be deactivated for the other elements. The

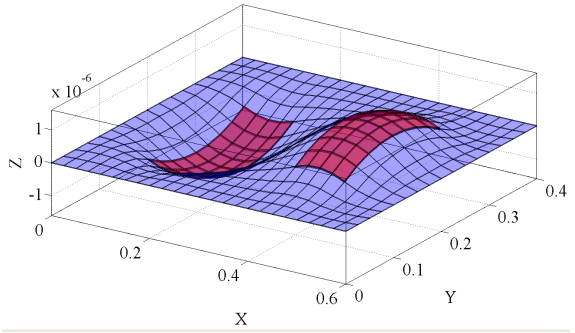

Figure 7. Static displacement obtained by ANCF

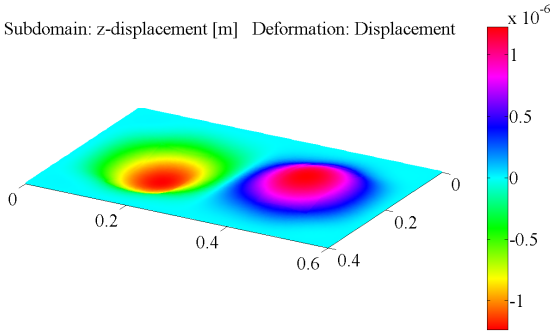

Figure 8. Static displacement distribution by COMSOL

plate boundaries are fixed supported. A static input voltage is applied to actuators elements at (8, 11,14 and 17) with the following magnitude:

$$\{\phi_a^i\} = \{10 \quad -10 \quad 10 \quad -10\}^T \tag{57}$$

As can be seen from Figure (7) and Figure (8), both the ANCF and the COMSOL® approaches give close results for the static displacement distribution.

4.2 Dynamic Analysis

For thin piezoelectric laminated rectangular plates with fixed supported boundary conditions, the present ANCF technique, and the software COMSOL® are used to calculate the total displacement distribution in z direction for the structure. Using the piezoelectric actuators/sensors configuration as shown in Figure (6). The comparison of the dynamic response of the plate due to the excitation caused by a voltage applied to the actuators as in Equation (57) with no mechanical loading at different time instants is shown in Figures (9,10) with very good agreement.

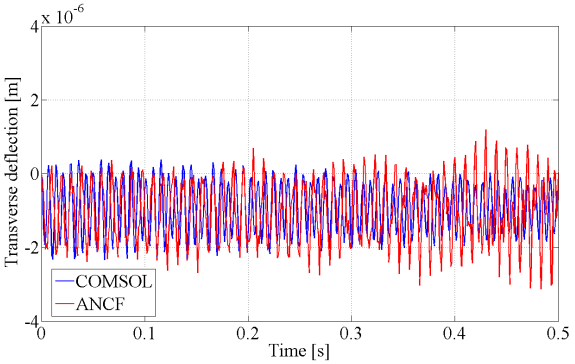

Figure 9. Comparison of the z-displacement of node (17)

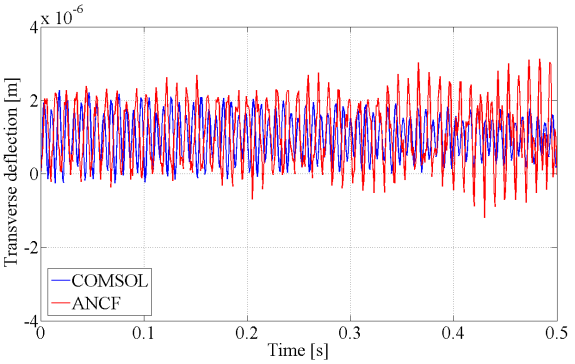

Figure 10. Comparison of the z-displacement of node (19)

4.3 Eigenfrequency Solution

A simplified calculation of the curvature is employed by supposing the normal vector $\{n\}$ to be fixed at $\{0 \quad 0 \quad 1\}^T$. In this case, Equation (11) gives the same curvatures and twist as in the linear case. In this case, the curvature vector can be defined as:

$$\{\kappa\} = [B]\{e\} \tag{58}$$

where the linear matrix $[B]$ can be defined as:

$$[B] = \begin{bmatrix} \{S_{xx}\}^T & \{S_{yy}\}^T & 2\{S_{xy}\}^T \\ {\scriptstyle (3,:)} & {\scriptstyle (3,:)} & {\scriptstyle (3,:)} \end{bmatrix}^T \tag{59}$$

where $\{S_{xx}\}$ is the 3^{rd} row of the second derivative of the shape function with respect to x. Therefore
$\scriptstyle (3,:)$
the stiffness matrix $\left[K^i_{ee}\right]$ should be linear in the nodal coordinates $\left\{e^i\right\}$. The linearized stiffness matrix, Equation (41) and the mass matrix, Equation (40) are used to calculate the eigenfrequencies of the piezoelectric laminated plate. A comparison with the COMSOL Eigen-Frequency Module is carried out, the first 10 eigenfrequences are shown in Table (2), Figures(11-18) shows the COMSOL® eigen-modes with the corresponding eigenfrequencies.

$Mode\ \#$	$COMSOL$	$ANCF$
1	78.71	79.881
2	103.30	102.13
3	202.41	199.41
4	207.64	201.40
5	217.52	212.02
6	281.24	270.87
7	361.84	348.11
8	435.62	417.73
9	474.36	501.48
10	519.11	583.64

Table 2. Comparison of eigen-frequencies $[Hz]$

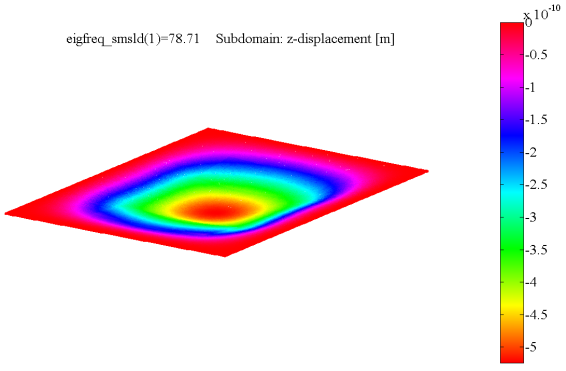

Figure 11. First mode

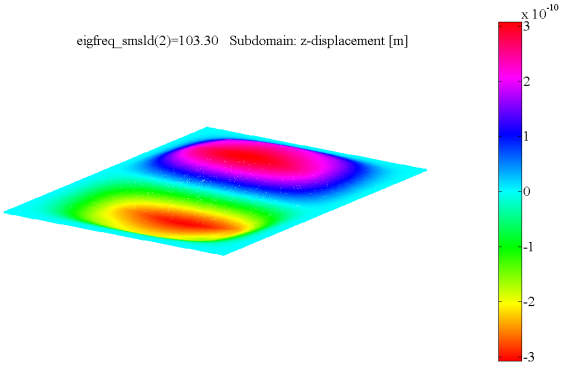

Figure 12. Second mode

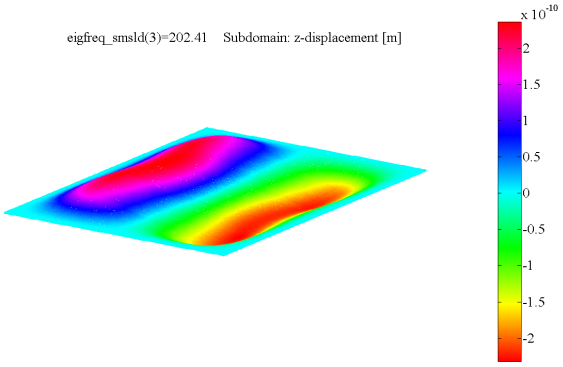

Figure 13. Third mode

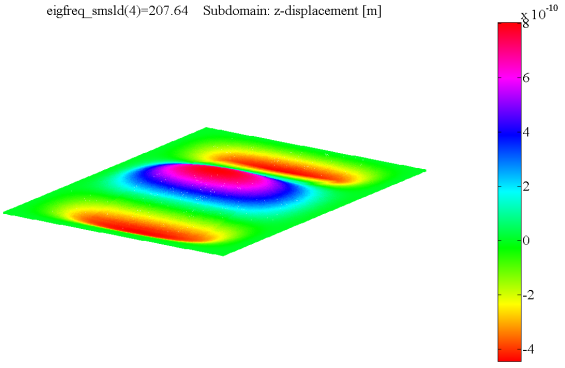

Figure 14. Fourth mode

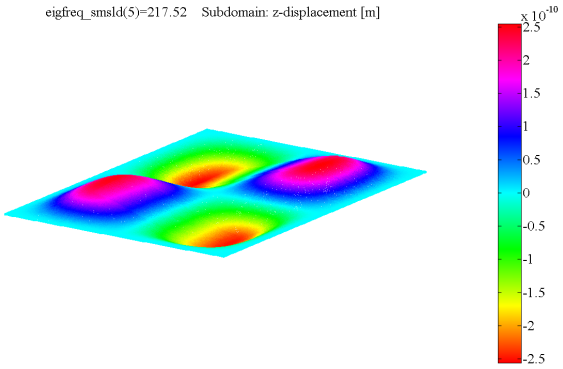

Figure 15. Fivth mode

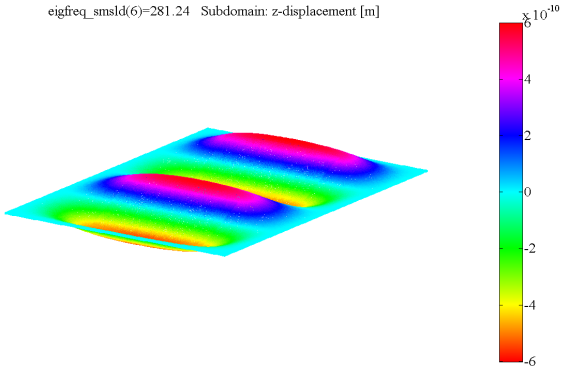

Figure 16. Sixth mode

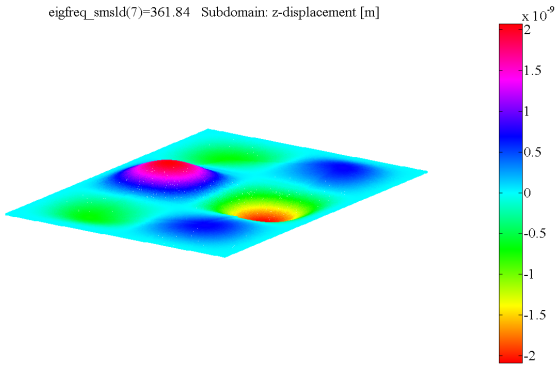

Figure 17. Seventh mode

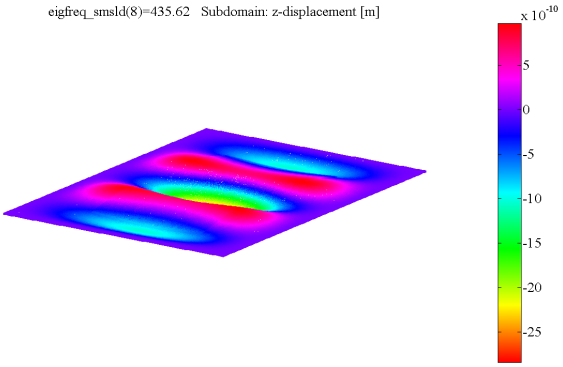

Figure 18. Eighth mode

5 CONCLUSIONS

A non-incremental finite element formulation based on Absolute Nodal Coordinate Formulation (ANCF) has been developed for the analysis of smart composite structures with piezoelectric materials. All important steps were presented in detail, in such a way that the modeling technique used can be easily understood. Besides, various computational tests were performed (static, dynamics and eigen-frequency) demonstrating the efficiency of the methodology used. Results were presented for a fixed supported rectangular thin plate excited and sensed by various rectangular actuators and sensors bonded symmetrically to both sides of the plate. The results for the static and dynamic analysis obtained by the present ANCF show good agreement with those solutions of the software COMSOL®. The present solutions are useful for understanding the electromechanical coupling in intelligent structures under dynamic conditions. Besides, the present methodology is useful for the design of vibration control devices.

REFERENCES

[1] Allik H., Hughes T.J., Finite element method for piezoelectric vibration. *International Journal for Numerical Methods in Engineering 2* (1970), 151-157.

[2] Benjeddou A. Advances in piezoelectric finite element modeling of adaptive structural elements: a survey. *Computers & Structures 76* (2000), 347-363.

[3] Carrera, E. Theories and finite elements for multilayered, anisotropic, composite plates and shells. *Archives of Computational Methods in Engineering 9* (2002), 87-140

[4] Carrera, E. A historical review of zig–zag theories for multilayered plates and shells. *Applied Mechanics Reviews 56* (2003), 287-308.

[5] COMSOL MULTIPHYSICS. http://www.comsol.com/

[6] Chattopadhyay, B., Sinha. P.K., Mukhopadhyay, M. Geometrically nonlinear analysis of composite stiffened plates using finite elements. *Composite Structures 31* (1995), 107-18.

[7] Dufva, K. and Shabana, A.A. Analysis of Thin Plate Structure Using the Absolute Nodal Coordinate Formulation. *IMechE Journal of Multi-body Dynamics 219* (2005), 345-355.

[8] Ha, S.K., Keilers, C., Chang, F.K. Finite element analysis of composite structures containing distributed piezoceramic sensors and actuators. *AIAA Jornal 30* (1992), 772-780.

[9] Hwang W.S., Park H.C. Finite element modeling of piezoelectric sensors and actuators. *AIAA Jornal 31* (1993), 930-937.

[10] Mackerle, J. Sensors and actuators: finite element and boundary element analyses and simulations a bibliography (1997–1998). *Finite Elements in Analysis and Design 33* (1999) 209-220.

[11] Mackerle, J. Smart materials and structures: FEM and BEM simulations a bibliography (1997–1999). *Finite elements in analysis and design 37* (2001), 71-83.

[12] Mackerle, J. Smart materials and structures-a finite element approach-an addendum: a bibliography (1997–2002). *Modelling and Simulation in Materials Science and Engineering 11* (2003),707-744

[13] Nada, A. A., Hussein, B. A., Megahed,S.M., Shabana A.A. Use of the floating frame of reference formulation in large deformation analysis: experimental and numerical validation. *Proceedings of the Institution of Mechanical Engineers, Part K: Journal of Multi-body Dynamic 224* (2010), 45-58.

[14] Nailon M., Coursant R.H.,Besnier, F. Analysis of piezoelectric structures by a finite element method. *ACTA Electron. 25* (1983), 341-362.

[15] Saravanos, D. A. and Heyliger, P. R. Mechanics and computational models for laminated piezoelectric beams, plates and shells. *Applied Mechanics Reviews 52* (1999), 305-320

[16] Shabana A.A. *Dynamics of Multibody Systems*, 3^{rd} ed. Cambridge: Cambridge University Press, 2005.

[17] Shabana A.A. *Computational Continuum Mechanics*, 3^{rd} ed. Cambridge: Cambridge University Press, 2008.

[18] Schwab A. L., Gerstmayr J., Meijaard J. P. Comparison of three-dimensional flexible thin plate elements for multibody dynamic analysis: finite element formulation and absolute nodal coordinate formulation. In *Proceedings of the ASME International Design Engineering Technical Conferences & Computers and Information in Engineering Conference* IDETC/CIE, 2007, Las Vegas, Nevada, USA

[19] Jian, P.J. and Dong, X. L. Finite element formulations for thermopiezoelastic laminated composite plates. *Smart Materials and Structures 17* (2008), 015027 (13pp).

[20] Zhang,Y.X. ,Yang C.H. Recent developments in finite element analysis for laminated composite plates. *Composite Structures 88* (2009), 147-157.